HHS Public Access

Author manuscript

Pflugers Arch. Author manuscript; available in PMC 2017 November 01.

Published in final edited form as:

Pflugers Arch. 2016 November ; 468(11-12): 2061–2074. doi:10.1007/s00424-016-1880-z.

Molecular mechanisms of inhibition on STIM1-Orai1 mediated Ca^{2+} entry induced by 2-aminoethoxydiphenyl borate

Ming Wei[*,1], **Yandong Zhou**[*,2], **Aomin Sun**[*,1], **Guolin Ma**[3], **Lian He**[3], **Lijuan Zhou**[1], **Shuce Zhang**[1], **Jin Liu**[1], **Shenyuan L. Zhang**[4], **Donald L. Gill**[2,#], and **Youjun Wang**[1,#]

[1]Beijing Key Laboratory of Gene Resources and Molecular Development, College of Life Sciences, Beijing Normal University, Beijing 100875, P.R. China

[2]Department of Cellular and Molecular Physiology, The Pennsylvania State University College of Medicine, Hershey PA 17033

[3]Institute of Biosciences and Technology, Texas A&M University Health Science Center, Houston, TX 77030, USA

[4]Department of Medical Physiology, College of Medicine, Texas A&M University Health Science Center, Temple, TX 76504, USA

Abstract

Store operated Ca^{2+} entry (SOCE) mediated by STIM1 and Orai1 is crucial for Ca^{2+} signaling and homeostasis in most cell types. 2-aminoethoxydiphenyl borate (2-APB) is a well described SOCE inhibitor but its action remains largely elusive. Here we show that 2-APB does not affect the dimeric state of STIM1, but enhances the intramolecular coupling between the coiled-coil 1 (CC1) and STIM-Orai Activating Region (SOAR) of STIM1, with subsequent reduction in the formation of STIM1 puncta in the absence of Orai1overexpression. 2-APB also inhibits Orai1 channels, directly inhibiting Ca^{2+} entry through the constitutively active, STIM1-independent Orai1 mutants, Orai1-P245T and Orai1-V102A. When unbound with STIM1, the constitutively active Orai1-V102C mutant is not inhibited by 2-APB. Thus we used Orai1-V012C as a tool to examine whether 2-APB can also inhibit the coupling between STIM1 and Orai1. We find that the functional coupling between STIM1 and Orai1-V102C is inhibited by 2-APB. This inhibition on coupling is indirect, arising from 2-APB's action on STIM1, and it is most likely mediated by gating residues in Orai1 N terminus. Overall, our finding of this two-direct-site inhibition may help better understanding of Orai1-activation by STIM1 and future drug design.

[#]Correspondence should be addressed to: Donald L. Gill, (dgill4@hmc.psu.edu) or Youjun Wang (wyoujun@bnu.edu.cn).
[*]These authors contributed equally to this work

Author Contributions

DLG and YW supervised and coordinated the study. SLZ provided Orai1-SS deletion mutants and intellectual inputs to the study. LH, GM and YZ designed and generated some plasmid constructs. MW, AS, LZ and YW performed confocal, Calcium, FRET and epifluorescence imaging. YW carried out the whole-cell patching. JL provided tech support for cell culture and confocal imaging. MW, AS, LZ, YW, and YZ analyzed data, with input from the other authors. SZ and SLZ helped with manuscript writing. YZ, YW and DLG wrote the manuscript.

Introduction

As a universal second messenger, Ca^{2+} mediates control over a wide spectrum of cellular activities (1, 2). In most cell types, store-operated Ca^{2+} entry (SOCE) is an important Ca^{2+} influx process mediating both Ca^{2+} signaling and homeostasis(3–6). STIM proteins and Orai channels are the two essential and sufficient mediators of SOCE. While the ER membrane protein STIM functions as a sensor that can sense the decreases in ER luminal Ca^{2+}, Orai is the calcium channel on plasma membrane (7). STIM, Orai and SOCE have been shown to correlate with many vascular and immune deficiency diseases and different types of cancer (3, 5, 8–10). Lots of important information regarding the molecular mechanisms that lead to Orai1 activation has been obtained recently (5, 11–14), yet the exact nature of this coupling and activation process still awaits further clarification.

Thus highly specific pharmacological tools targeting this process are needed, to better dissect the underlining molecular mechanism of SOCE, to more thoroughly examine its physiological or pathological roles, or for the purpose of disease therapy. So far many modifiers of SOCE have been found. However, most of these available inhibitors have flaws as they fail in one or more of the following criteria: highly specific, fast acting and reversible (reviewed in (15, 16)). One hinderance of developing better pharmacological tools is the lack of understanding of the currently available inhibitors. As the most characterized modulators of SOCE, 2-APB has been shown to enhance SOCE activity at 5–10 μM yet blocking it at 50 μM (17–23). However, the molecular basis for its actions on SOCE largely remains elusive.

We thus focused our current study on dissecting the underlining molecular mechanisms of SOCE inhibition by 2-APB (50 μM). Our results show that, in addition to its direct inhibition on Orai1 channels, 2-APB can also directly inhibit STIM1 protein by enhancing intramolecular interactions between the CC1 and SOAR region of STIM1. This inhibition on STIM1 leads to the reduction of STIM1 puncta formation in native HEK293 cells when Orai1 is not co-expressed. 2-APB did not directly inhibit the coupling between STIM1 and Orai1, while its actions on STIM1 may lead to an indirect inhibition on STIM1-gating of Orai1.

Methods

DNA constructs, cell culture and transfection

CFP-Orai1-V102C was generated from CFP-Orai1 by PolePolar Biotechnology Co., LTD (Beijing, China). Truncations CFP-Orai1-V102C-ΔC2 (ΔT266-A301) and CFP-Orai1-V102C -ΔN2 (ΔM1- K85) were then correspondingly generated from CFP-Orai1-V102C by the same company. Orai1-V102A-CFP was generated from Orai1-CFP by TransGen Biotech (Beijing, China). Orai1-L81N-CFP, Orai1-L81N-V102C-CFP, Orai1-K85E-V102C-CFP, CFP-Orai1-V102A-ΔC2 and CFP-Orai1-V102A were made by point mutations from corresponding Orai1 or Orai1-V102C mutant (TransGen Biotech, Beijing, China). Orai1-P245T-CFP was made from Orai1-CFP using the QuikChange Lightning site-directed mutagenesis kit (Agilent).

Cell culture and makings of stable cells: wild type Human embryonic kidney 293 (HEK wt) cells were maintained in regular DMEM (HyClone) supplemented with 10% FBS (Cleson Scientific), penicillin and streptomycin (Thermo Scientific) at 37 C with 5% CO_2 as previously described (24). HEK cells stably expressing Orai1-V102C-CFP, STIM1-YFP were generated by electroporation using the pires-Orai1-V102-CFP or MO91-STIM1-YFP construct and then selected with 100 μg/ml G418 (Invitrogen) or 2 μg/ml puromycin (Invitrogen) correspondingly (24). HEK stable cells co-expressing STIM1-YFP and Orai1-CFP or Orai1-V102C-CFP cells were generated by introducing STIM1-YFP into Orai1-CFP or Orai1-V102C-CFP stable cells using similar protocols. For HEK stable cells expressing Orai1 or Orai1-V102C, they were maintained in the above-mentioned medium supplemented with 100 μg/ml G418; for HEK STIM1-YFP cells, the extra supplement is 2 μg/ml puromycin; while for stable cells co-expressing two proteins, both puromycin and G418 were added in culturing medium.

Transfection of Plasmids was done with Polyethylenimine (PEI, Polysciences, Inc., Cat# 23966) (25) following manufacturer's protocol. The DNA to PEI ratio used was 1:2 one day after cells were seeded on a 25mm round coverslip with 70% confluence. All imaging experiments were performed one or two days after transfection.

Single-cell intracellular Ca^{2+} measurements

Intracellular Ca^{2+} signals shown by Fura-2 indicator were recorded using a ZEISS oberserver-A1 microscope equipped with a Lambda DG4 light source (Sutter Instruments), Bright line FURA2-C-000 filter set (Semrock Inc.), a 40× oil objective (NA = 1.30), an iXon3 EMCCD camera (Oxford Instruments), and the MetaFluor software (Molecular Devices).

Protocols for the loading of Fura-2 AM were similar to those described before (13): HEK293 cells were first kept in the imaging solution with 1 mM $CaCl_2$ and 2 μM Fura-2 AM for 30 min. Next, cells were kept in Fura-2 AM free imaging solution with 1 mM $CaCl_2$ for another 30 min. Collection of Fura-2 signals: Emission fluorescence at 509 nm generated by 340nm excitation light (F_{340}) and 380nm light (F_{380}) was collected every two seconds, and intracellular Ca^{2+} levels are shown as F_{340}/F_{380} ratio.

The imaging solution consists of (mM): 107 NaCl, 7.2 KCl, 1.2 $MgCl_2$, 11.5 glucose, 20 HEPES-NaOH (pH 7.2). Dependent on specific design of each experiment, different amount of $CaCl_2$ and other types of reagents were also included in imaging solution. For cells transfected with constructs that has constitutive Ca^{2+} influx, either 1mM Ca^{2+} with 10μM $GdCl^3$, 100~300 μM Ca^{2+} or nominally Ca^{2+} free solution were used to keep cells healthy. All experiments were carried out at room temperature. Traces shown are representative of at least three independent repeats with each including 15–60 single cells.

Fluorescence and Förster Resonance Energy Transfer (FRET) imaging

For FRET measurements, necessary calibrations and offline analysis were performed as described before (13). Briefly, raw images (F_{CFP}, F_{YFP} and F_{raw}, respectively) were collected every 10 sec using the above-mentioned imaging system equipped with an Optosplit II Image Splitter (Cairn Research Limited) and the following three filters: CFP

(428.9±5.5$_{Ex}$/465±32$_{Em}$), YFP (502.6±11.2$_{Ex}$/549±21$_{Em}$), and FRET$_{raw}$ (428.9±5.5$_{Ex}$/549±21$_{Em}$). After readings from raw images were obtained, three channel corrected FRET was first calculated using this formula: $FRET_c = F_{raw} - F_d/D_d * F_{CFP} - F_a/D_a * F_{YFP}$, where $FRET_c$ represents the corrected total amount of energy transfer, and F_d/D_d represents measured bleed-through of CFP into the FRET filter (0.84), F_a/D_a represents measured bleed-through of YFP through the FRET filter (0.13). Second, N-FRET (normalized FRET) was calculated by normalizing $FRET_c$ values against donor fluorescence (F_{CFP}) to reduce variations caused by differences in expression levels. Third, apparent FRET values, E_{app}, was calculated using the following equation: E_{app}= N-FRET/(N-FRET+G), where G (4.59) is the system-dependent factor. YFP-STIM1-D76G-F394H-CFP expressed in HEK293 cells was used as a calibrator of relative expression levels of CFP- and YFP-tagged proteins. Also, it served as a negative control in our experiments, since YFP and CFP of this probe is separated by ER membrane with a distance more than 10 nm (26). To minimize fluctuations in Eapp caused by variations in expression ratios of donor protein to acceptor protein, only cells with F_{CFP}/F_{YFP} ratio falling between 0.5 ~ 1 were used for data analysis. All fluorescence images were collected and processed with MetaFluor software (Molecular Devices), and the resulting data were further analyzed with Matlab R2012b software and plotted with Prism5 software. Representative traces of at least three independent experiments are shown as mean ± s.e.m.

Unless specified, fluorescence images or figures showing cellular distribution of E_{app} were obtained with a Zeiss observer Z1 fluorescence microscope Controlled by Zen Software. CFP, YFP images were collected with 40 X oil objective (N.A. 1.3) and corresponding Semorock Bright line filter sets (CFP-2432C-000, YFP-2427B-000). And a re-combination of the above filter sets was used to collect raw FRET images, with the excitation filter from CFP filter set, while the dichroic and emission filter from YFP filter set. Cellular E_{app} images were generated by executing a Zeiss-made macro in Zen software using the same calibration methods and the following parameters: F_d/D_d = 0.37; F_a/D_a =0.18; G = 2.94.

Confocal microscopy and puncta analysis

Images of some experiments examining co-localization between proteins or STIM1 puncta were taken with a ZEISS LSM700 confocal microscope equipped with 100X oil objective (N. A. 1.6), 405nm and 488nm laser, controlled by Zen software.

To calibrate bleed through between different channels, besides cells co-expressing both YFP- and CFP-tagged proteins, fluorescence images of cells expressing only either CFP- or YFP-tagged proteins were also collected with the same parameters as those used for co-expressing cells. Then bleed through factors were calculated off-line with ImageJ software. And the co-localization images shown were bleed-through corrected.

Puncta analysis was done with a customized macro plug-in of ImageJ software modified from a previously published protocol (27). Briefly, Type of puncta images was first converted from 16bit to 8bit, and then background was subtracted using a rolling ball with a radius larger than 15 pixels. Second, the resulting images were converted to binary images, and then further treated with “watershed” function. Third, statistics of puncta were then obtained with “Analyze particles” function in ImageJ. Only particles with a size larger than

4 pixels were taken as puncta. The macro file used for puncta analysis is available upon request.

Electrophysiology

Electrophysiological measurements were taken using conventional whole-cell patch clamp using cells grown on glass coverslips as described previously (28). At a holding potential of 0 mV, linear voltage ramps of 50 ms duration spanning from −100 to +100 mV were delivered at a rate of 0.5 Hz immediately following the establishment of the whole-cell configuration. The pipette solution contained (mM): 145 CsGlu, 10 HEPES, 10 EGTA, 8 NaCl, 6 $MgCl_2$, 2 Mg-ATP (pH 7.2). 8 mM Mg^{2+} and ATP were used to inhibit TRPM7 current. For Experiments performed in Orai1-V102C stable cells, 3mM $CaCl_2$ was added to make the free Ca^{2+} concentration 100nM. The extracellular solutions contained (mM): 145 NaCl, 10 CaCl2, 10 CsCl, 2 MgCl2, 2.8 KCl, 10 HEPES, 10 glucose (pH 7.4). A 10 mV junction potential compensation was applied.

Results

2-APB enhanced interactions between STIM1-CC1 and SOAR, which is essential and sufficient for its inhibition on STIM1 puncta

When ER Ca^{2+} stores are full, STIM1 molecules are uniformly distributed over the entire ER membrane. Upon store depletion, STIM1 forms puncta and activates Orai1 channels (5). High concentration (50 μM) of 2-APB, a powerful SOCE modifier, can block or reverse the formation of STIM1 puncta and it was proposed that such reduction of puncta mediated the inhibition on SOCE (20, 21). However, the exact mechanisms by which 2-APB affects puncta are still not known. We addressed this question by examining the effects of 2-APB on several known critical steps involved in the formation of STIM1 puncta.

Initially, we tested whether 2-APB has any effect on STIM1-STIM1 interactions. Following store depletion, the dissociation of Ca^{2+} ions from the EF hand within the STIM1 ER-luminal region triggers dimerization of the luminal domain (29). Thus we examined FRET signals between the C-terminally truncated STIM1-(1-237) fragment containing the entire ER-luminal and TM region of STIM1. Our results showed that 2-APB had no effect on FRET signals between CFP- and YFP-tagged versions of these STIM1 fragments, regardless of whether the ER store was full or depleted (Fig. 1A). These results indicate that 2-APB does not affect the dimeric state of the entire ER and TM region of STIM1. Next, we examined whether interactions between STIM1 cytosolic fragments were affected by 2-APB. The entire cytosolic C-terminal doman (STIM1ct), or just the STIM1-Orai1 Activating Region (SOAR) or CRAC-Activating Domain (CAD) of STIM1, each exist as cytosolic dimers when expressed (reviewed in (5)). Indeed, the SOAR/CAD region of STIM1 is essential for oligomerization and puncta formation of STIM1 (30, 31). Our results show that 2-APB does not induce any significant changes in FRET signals between STIM1ct (Fig. 1B) or SOAR molecules (Fig. 1C), regardless of whether FRET signals were measured when they were Orai1-bound or free in the cytosol (Fig. 1C). Thus 2-APB does not directly alter cytosolic STIM1-STIM1 interactions. 2-APB also did not have any effect on FRET signals

between YFP-STIM1 and CFP-STIM1 (Fig. 1D). Together, these results indicate that 2-APB does not inhibit STIM1 puncta by disrupting inter-molecular interactions of STIM1.

We then examined whether 2-APB can block the intra-molecular interactions that occur during STIM1 activation using a two-component system consisting of STIM1-(1-310)-CFP and YFP-SOAR. This two-component system has been successfully applied to report interactions between STIM1-CC1 and SOAR using co-localization or FRET imaging (13). We tested the effects of 2-APB on the coupling of STIM1-CC1 and SOAR with this system. When co-expressed in HEK cells, STIM1-(1-310)-CFP and YFP-SOAR co-localize (Fig. 1E, top row) and have high FRET signals at rest (Fig. 1H). Upon store depletion with ionomycin, SOAR was uncoupled from ER-localized STIM1-(1-310) and became evenly distributed in cytosol (Fig. 1E, middle row)), resulting in diminished FRET signals (Fig. 1H). After the application of 50 μM 2-APB, SOAR moved back to the ER and co-localized with STIM1-CC1 again (Fig. 1E, bottom row). As a result, the ionomycin-induced decrease in FRET signal was partially reversed by 2-APB (Fig. 1H). These results indicate that 2-APB could induce coupling between STIM1-CC1 and SOAR, and the enhanced coupling between STIM1-CC1 and SOAR could partially recover the FRET decrease caused by store depletion. Therefore, 2-APB could induce or enhance interactions between STIM1-CC1 and SOAR, locking STIM1 into its resting, inhibitory state.

To test whether those critical residues, essential for interactions between STIM1-CC1 and SOAR, are also required for 2-APB's actions on puncta, we examined 2-APB's effects on interactions between corresponding mutants of STIM1-(1-310) or SOAR. Both STIM1-(1-310)-L258G or SOAR-L416G mutations have been previously shown to disrupt interactions between STIM1-CC1 and SOAR (13) (Fig. 1F&G). When examined with co-localization imaging, 2-APB also failed to dock SOAR-L416G back to ER-localized STIM1-CC1 (Fig. 1F), or restore the docking of SOAR back to STIM1-(1-310)-L258G (Fig. 1G). These mutants also abolished 2-APB's ability to restore FRET signals between SOAR and STIM1-(1-310) (Fig. 1H). These results show that 2-APB's actions on STIM1 require these critical residues that are essential for the coupling between STIM1-CC1 and SOAR.

To test whether the enhanced coupling between STIM1-CC1 and SOAR is sufficient for the inhibition of puncta by 2-APB, we examined the effects of 2-APB on puncta formed by STIM1 and various mutants (Fig. 2A–B). Similar to previous reports (20, 21), 2-APB can reduce puncta formed by wt STIM1 after store depletion (Fig. 2A, top row). 2-APB did not significantly reduce the number of puncta (Fig. 2B, upper), it reduced the average size of puncta instead (Fig. 2B, lower). The D76A mutation in the EF hand of STIM1 causes the loss of Ca^{2+} binding, resulting in the formation of constitutive puncta (27) (Fig. 2A, 2nd row). Application of 50 μM 2-APB could largely inhibit puncta of YFP-STIM1-D76A. However, constitutive puncta formed by STIM1-L258G (Fig. 2A, third panel from top) or STIM1-L416G (Fig. 2A, bottom panel) were unaffected by 2-APB. Therefore, 2-APB's inhibitory effect on STIM1 puncta is dependent on residues critical for interactions between STIM1-CC1 and SOAR. The enhanced interactions between STIM1-CC1 and SOAR (residue 344-442) are essential and sufficient for 2-APB's inhibition on STIM1 puncta.

2-APB's inhibitory effect on STIM1 is not essential for the inhibition of SOCE

2-APB inhibits SOCE at high concentrations (15, 16), and the disruption of STIM1 puncta by 2-APB was proposed to explain its inhibition on Ca^{2+} influx through Orai1 channels (21). However, there have been some discrepancies regarding 2-APB's ability to inhibit STIM1 puncta (20, 32, 33). We thus examined whether the inhibition of puncta and of SOCE represent the same mechanism or can be separated. We examined this by comparing 2-APB's effects on SOCE and puncta in HEK wt cells expressing STIM1 or mutants thereof (Fig. 2A–C). In cells expressing either wt STIM1 or STIM1-D76A, both of which contain intact CC1-SOAR interactions, 2-APB reduced the punctate area similarly (Fig. 2A, top two rows). 2-APB did not inhibit puncta formed by the STIM1-L258G or STIM1-L416G mutants with no CC1-SOAR interactions (Fig. 2A, bottom two panels). However, whether STIM1 puncta were inhibited or not, SOCE was inhibited similarly in all groups (Fig. 2C). Therefore, 2-APB's actions on STIM1 puncta and its inhibitory effect on SOCE can be separated in HEK wt cells overexpressing STIM1 or its mutants.

We also directly compared the effects of 2-APB on STIM1 puncta and SOCE in cells with or without co-expression of Orai1 channels. We performed these experiments with two types of cells seeded on the same cover slip: cells overexpressing STIM1-YFP only or cells co-expressing both STIM1-YFP and Orai1-CFP. In STIM1-YFP cells, 2-APB greatly reduced the punctate area of STIM1 (Fig. 2D, "green" cell on the left). However, in STIM1-YFP-Orai1-CFP double expressing cells, STIM1 puncta were unaffected by 2-APB (Fig. 2D, "orange" cell on the right). This result indicates that Orai1-coupling with STIM1 can mask the inhibitory effect of 2-APB on STIM1. 2-APB's failure to inhibit STIM1 puncta in STIM1-Orai1 cells may be due to its enhancing effects on the coupling between STIM1ct and Orai1 (23). Even though 2-APB's ability to reduce STIM1 puncta is abolished in HEK STIM1-Orai1 cells, it could still greatly inhibit SOCE (Fig. 2E). Therefore, the inhibition of SOCE can clearly be separated from the disruption of STIM1 puncta in cells co-expressing Orai1.

Overall, with either co-expression of Orai1 or with mutations disrupting interactions between STIM1-CC1 and SOAR, we show that 2-APB can inhibit SOCE independently of effects on STIM1 puncta. Therefore, the inhibition on SOCE by 2-APB was not affected by abolishing its effect on the coupling between STIM1-CC1 and SOAR (Fig. 2A–C). We further examined this phenomenon using constructs based on the SOAR molecule as opposed to intact STIM1. First, we examined the effects of 2-APB on constitutive Ca^{2+} influx in HEK Orai1 cells co-expressing SOAR-L416G. The SOAR-L416G molecule has no CC1 region and its L416 residue critical for CC1-SOAR interaction is mutated to a non-functional glycine and is thereby devoid of inhibition by 2-APB. Similar to cells co-expressing Orai1 and wildtype SOAR, (24, 28), 2-APB did not appear to physically uncouple SOAR-L416G and Orai1 as there was no decrease in FRET signals Instead, we observed that 2-APB enhanced the FRET signals between Orai1 and SOAR-L416G (Fig. 2F, left trace). Moreover, even with its inhibitory effect on SOAR missing, 2-APB could still greatly inhibit the constitutive Ca^{2+} entry (Fig. 2F, right trace).

Second, we checked the effects of 2-APB on Orai1-SS, a construct with one Orai1 subunit fused with one SOAR (336-485) dimer (34, 35). The SOAR dimer also does not have the

CC1 region that is critical for the binding of SOAR, and it is unable to form heteromers with the CC1 region of native STIM1 (13), thus it cannot be inhibited by 2-APB. We observed that 2-APB similarly inhibited the constitutive Ca^{2+} influx in HEK cells overexpressing Orai1-SS, Orai1-SS-ΔN1 (Δ1-73), or Orai1-SS-ΔC1 (Δ277-301) (Fig. 2G). Taken together, after the removal of 2-APB's inhibition sites, 2-APB can still inhibit constitutive Ca^{2+} entry induced by these STIM1 mutants. Therefore, 2-APB's inhibitory effect on STIM1, or its enhancing effect on the coupling between STIM1-CC1and SOAR, are not essential for the inhibition of Ca^{2+} influx through STIM1-activated Orai1 channels. In other words, 2-APB can inhibit SOCE through sites other than those identified in the STIM1 molecule.

2-APB modifies Ca^{2+} entry mediated by constitutively active Orai1 mutants, independently of STIM1

Since SOCE is mediated by both STIM1 and Orai1, the inhibition of SOCE by 2-APB could occur at the level of STIM1, Orai1 or STIM1-Orai1 coupling. With 2-APB's inhibitory sites on STIM1 identified and their non-essential role in the inhibition of SOCE established, we then examined possible actions of 2-APB on Orai1 channels.

Normally, Orai1 channels are inactive at rest (Fig. 3A), and they become active through the coupling of STIM1. Thus it is not possible to dissect the inhibitory actions of 2-APB on wt Orai1 in a STIM1 free background. However, Orai1 mutants have been identified which are constitutively active even without the coupling of STIM1 (14, 36, 37). These mutants make it possible for the direct assessment of 2-APB's effect on Orai1 channels.

Initially we examined the effects of 2-APB on the Ca^{2+} entry mediated by constitutive Ca^{2+} influx through Orai1-P245T mutant (37), and it was also inhibited by 2-APB (Fig. 3B). Similarly, Ca^{2+} entry via Orai1-V102A mutant (36) was also inhibited by 2-APB (Fig. 3C). Moreover, this inhibition is unaffected by either co-expression of STIM1, or deletion of its c-terminus (267-301) to abolish its ability to bind STIM1 (35) (Fig. 3C–D). Thus this inhibition is independent of STIM1, indicating a direct inhibition on Orai1 channels.

Interestingly, 2-APB totally lost its ability to inhibit Ca^{2+} entry through a different V102 mutant, Orai1-V102C (36)(Fig. 3E–G). In HEK cells stably expressing Orai1-V102C, the resulting constitutive Ca^{2+} entry (Fig. 3E) or whole cell current (Fig. 3F) was transiently enhanced by 2-APB. Similar enhancing effects were seen in cells co-expressing STIM1 and Orai1-V012C, or in cells expressing Orai1-V102-ΔC2, a mutant that loses its ability to bind STIM (35) (Fig. 3G).

2-APB's actions on STIM1 contributes to its inhibition on SOCE

When not bound with STIM1, constitutively active Orai1-V102C was not inhibited by 2-APB (Fig. 3E–G), making it a perfect tool to dissect possible inhibitions of 2-APB on STIM1-Orai1 coupling. We thus examined the effects of 2-APB on Orai1-V102C that were coupled with STIM1. After store depletion, SOCE mediated by STIM1 and wt Orai1 was first transiently activated, then rapidly inhibited by 2-APB (16, 18)(Fig. 4A). While in cells co-expressing Orai1-V012C and STIM1, when examined with Ca^{2+} imaging, the transient activation phase on SOCE was greatly enhanced and prolonged. And the inhibitory effect by 2-APB is not really visible (Fig. 4B). However, a slight inhibition on I_{CRAC} could be seen

when measured with whole-cell patch clamp, a more accurate method to assess SOCE (Fig. 4C). After about 4 min in 2-APB, the removal of 2-APB could induce an immediate increase in whole-cell current, indicating an inhibition around 25% (Fig. 4C). While there was no such effect in HEK Orai1-V102C cells with a fully-filled store (Fig. 3F). Therefore, after store depletion, the binding of STIM1 to Orai1-V102C makes it accessible to the inhibition of 2-APB.

This inhibition on STIM1-bound Orai1-V102C could either be induced by 2-APB's effects at the level of STIM1 or on the coupling between STIM1 and Orai1-V102C. We first tried to check 2-APB's effects in cells co-expressing Orai1-V102C together with various constitutive active, full length STIM1 mutants. Our attempt failed as cells co-expressing both proteins all died, probably due to toxic effect induced by high cytosolic Ca^{2+} levels. We then examined the effect of 2-APB in HEK cells co-expressing Orai1-V102C and SOAR-L416G, a mutant that devoid of 2-APB's inhibition on STIM1. The constitutive Ca^{2+} entry mediated by Orai1-V102C and SOAR-L416G was not affected by 2-APB even after 5 min incubation (Fig. 4D). This result indicates that, 2-APB's actions on STIM1-CC1 and SOAR are essential for its inhibition on STIM1-bound Orai1-V102C.

To gain some insights regarding how this enhanced coupling between STIM1-CC1 and SOAR could inhibit Ca^{2+} entry through STIM1-bound Orai1-V102C, we checked whether 2-APB can affects the coupling between STIM1 and Orai1-V102C with FRET imaging. In HEK cells stably co-expressing STIM1 and Orai1-V102C, store depletion induced an increase in FRET signals between STIM1 and Orai1-V102C. This FRET signal was then further increased by 2-APB (Fig. 4E). Similar results obtained with wt Orai1 and activated-STIM1 or its cytosolic fragments were also reported previous (23, 24, 28, 32). This result indicates that 2-APB's enhancing actions on STIM1-CC1 and SOAR are not enough to break the existing coupling between STIM1 and Orai1-V102C. We then examined whether 2-APB pre-incubation can inhibit the development of STIM1-coupling with Orai1 during the process of store depletion. Even though it didn't reduce the maximal FRET signals between STIM1 and Orai1-V012C, pre-incubation with 2-APB greatly slowed down the increase rate of FRET signals (Fig. 4F). Similarly, pre-incubation with 2-APB also greatly delayed the formation of STIM1 puncta (Fig. 4G). Overall, these results indicate that the enhanced coupling between STIM1-CC1 and SOAR, induced by 2-APB, was too weak to block or disrupt the physical coupling between STIM1 and Orai1-V102C (Fig. 4E–G). However, pre-incubation with 2-APB did slowed down the coupling of STIM1 to Orai1-V102C (Fig. 4F&G).

Since its inhibitory effect on the coupling STIM1 to Orai1-V102C was more detectable when 2-APB was applied before store depletion, we then examined whether 2-APB could inhibit SOCE in a similar manner. Indeed, even though pre-incubation with 2-APB doesn't inhibit the constitutive Ca^{2+} entry when ER Ca^{2+} store is full (Fig. 4H), it can inhibit Ca^{2+} entry through Orai1-V102C after store depletion (Fig. 4I). And if 2-APB was applied before store depletion with ionomycin, 5 min incubation with 2-APB inhibited SOCE by 76.6 ± 3.2 %. However, if 2-APB was applied after the store was fully depleted, its inhibition on SOCE was significantly less (57.1 ± 5.1%, p=0.002, t-test) (Fig. 4I). Thus the extent of 2-

APB's inhibition on SOCE correlates with its ability to affect the coupling between STIM1 and Orai1-V012C.

Therefore, 2-APB's inhibition on STIM1-bound Orai1-V102C channels is mediated by its enhanced auto-inhibition of STIM1. And its inhibitory effect on STIM1 is not strong enough to physically disrupt the coupling between STIM1 and Orai1-V102C complex (Fig. 4E). It is very likely that this 2-APB&STIM1 dependent inhibition is mediated through disruptions of the functional coupling between STIM1 and Orai1-V012C.

The inhibition of 2-APB on STIM1-bound Orai1-V102C is abolished by K85E mutation at Orai1 N-terminus

Even though recent evidences show both N and C terminus of Orai1 are involved in channel gating and its coupling with STIM1(14, 28, 38–40) (41–43), C-terminus of Orai1 involves more in STIM1-binding(32, 34, 35, 44), while its N-terminus may be more crucial for channel gating(5, 35, 45, 46). More specifically, the ETON region (Extended Transmembrane Orai1 N-terminal, AA73–90) has been shown to be essential for STIM1-binding and channel gating (38, 47). As a critical residue in ETON region, Orai1-K85E mutant was proposed as a gating residue for Orai1 channels (45). Later on, it was shown to also have impaired binding with Orai1 or Orai1-V102C (38, 39) (45).

We therefore checked whether K85E mutation in ETON region could affect the inhibition of 2-APB on SOCE mediated by STIM1-bound Orai1-V102C. Similar to previous report (39), Orai1-K85E-V102C mutant still remains constitutively active (Fig. 5A&B). Even though it has impaired binding with STIM1, it can couple with STIM1 and become further activated after store depletion (Fig. 5C) (39). When 2-APB was added after the application of Ca^{2+}, the Ca^{2+} entry through Orai1-K85E-V102C channels are enhanced by 2-APB, no matter when it is STIM1-free (or store full) or it is STIM1-bound (or store depleted) (Fig. 5B). When 2-APB was applied 5 min before the addition of Ca^{2+}, both constitutive Ca^{2+} influx and SOCE were still enhanced by 2-APB (Fig. 5D&E). Thus K85E mutation abolished 2-APB's inhibition on STIM1-bound Orai1-V102C (Fig. 5E vs Fig. 4I), even though pre-incubation with 2-APB could still slow the rate of increase in FRET signals between STIM1 and Orai1-K85E-V102C, indicating that 2-APB's inhibitory effect on STIM1 is still intact (Fig. 5F). Therefore, K85 serves as a critical link, relaying 2-APB's inhibitory effect on STIM1, to the opening of Orai1-V102C. Thus the ETON region is essential to mediate 2-APB's inhibition on STIM1-bound Orai1-V102C. More studies are needed to examine whether the corresponding region in Orai2 or Orai3 also mediates 2-APB's inhibition on STIM1-bound Orai2 or Orai3.

Discussion

SOCE mediators, including STIM1-2 proteins and Orai1-3 channels, and SOCE Ca^{2+} signals have been shown to be crucial for many cellular responses(4, 5, 48, 49), to have many important physiological roles and involved in different types of diseases(8, 49). Thus there is a great need to develop highly isoform- and tissue-specific inhibitors of SOCE, to better understand the exact physiological or pathological roles of different isoforms of STIM and Orai, and eventually for disease-treatments. Even with the guidance of solved crystal

structure of Orai1 and SOAR (43, 50), drug development is still at its preliminary stage, and the underlining molecular mechanisms for most SOCE inhibitors still remain largely undefined (15, 16). As one of the most used SOCE modifiers, 2-APB enhances SOCE at low concentrations and inhibits SOCE after a transient activation at higher concentrations (17, 18). And its actions on CRAC activity, that are mediated by different isoforms of STIM and Orai, has been intensively examined (15–23, 32, 51). However, current understandings of the molecular basis of its actions are mainly constrained on its activations (22, 23, 52–57), while the possible mechanisms of its inhibitory effects were poorly understood (15, 16, 21).

The results here reveal that 2-APB could inhibit SOCE by directly working on the two essential mediators of SOCE, STIM1 and Orai1. The geometry of the Orai1 pore is critical for the direct inhibition of 2-APB, and this fast-developing inhibition on Orai1 channels is usually 90% complete within 90 sec (Fig. 3B&C). Similarly, 2-APB's direct inhibition on STIM1 also fully develops within several minutes (Fig. 1H). 2-APB inhibits STIM1 by enhancing or inducing coupling between its CC1 and SOAR region, thus locking STIM1 to its auto-inhibitory, resting state. Aside from its direct actions on Orai1 and STIM1, 2-APB can also indirectly inhibit the functional coupling between STIM1 and Orai1 via its actions on STIM1, probably by weakening the interactions between STIM1 and the Orai1 N-terminal ETON region. This STIM1-dependent, indirect effect develops slower that 2-APB's direct actions on STIM1 (Fig. 1H vs Fig. 4C&H). This slower action is probably caused by the enhanced coupling between Orai1 and STIM1 or STIM1ct (23, 32) (Fig. 4E).

Store depletion leads to the formation of STIM1 puncta and the physical coupling of STIM1 to Orai1. And there has been some controversy on 2-APB's ability to inhibit STIM1 puncta (20, 21, 32, 33). Briefly, STIM1 puncta transiently expressed in HEK wt cells were shown to be greatly inhibited by 2-APB (20, 21). While there were also reports showing that, in HEK cells expressing STIM1 together with Orai1, 2-APB's ability to inhibit STIM1 puncta is either severely impaired or abolished (20, 32, 33). It is still unclear whether this discrepancy is an Orai1 effect or not. By imaging STIM1 cells with or without co-expression of Orai1 under the same view field, we clearly demonstrate that most of this discrepancy is caused by the differences in the amount of Orai1 used in different labs (Fig. 2D): co-expression of Orai1 together with STIM1 will abolish 2-APB's ability to inhibit STIM1 puncta. Based on this observation and these previous reports (20, 21, 28, 32, 33), we propose a "push and pull" model to explain whether STIM1 puncta can be inhibited by 2-APB or not. Briefly, 2-APB has two antagonizing, "push and pull" effects on STIM1: its direct actions on the CC1 and SOAR region of STIM1 will pull STIM1-SOAR region back toward ER to lock STIM1 in its resting state, thereby inhibiting the formation of STIM1 puncta (20, 21); while its Orai1-dependent enhancing effects on the coupling between STIM1 and Orai1 (23, 28, 32, 33) will push STIM1-SOAR region toward PM, keeping STIM1 in its activated, punctate distribution (Fig. 2D). And the Orai1-dependent pushing effect of 2-APB is stronger than its pulling effect on STIM1, thus 2-APB cannot disrupt established STIM1-Orai1 interactions. Instead, it enhances FRET signals between Orai1 and STIM1 or STIM1 fragments (23, 28, 32) (Fig. 4E).

Overall, those punctate area formed by Orai1-bound STIM1 are resistant to 2-APB, while Orai1-free STIM1 puncta can be abolished by 2-APB. Thus according to this model, the

ability of 2-APB to inhibit wt STIM1 puncta depends on the relative amount of STIM1 that are unbound with Orai1. In HEK wt cells overexpressing STIM1, endogenous Orai1 can only keep limited amount of STIM1 molecules in their punctate distributions. While the majority of punctate area are formed by Orai1-free STIM1, thus can be abolished by 2-APB (Fig. 2A). As a result, 2-APB can reduce STIM1 puncta the most in HEK STIM1 cells. While when moderate amount of Orai1 is also co-expressed with STIM1, most STIM1 will be bound to Orai1 after store depletion. Thus only a small portion of STIM1 molecules are not bound with Orai1 and these puncta can be abolished by 2-APB, resulting partial inhibition of STIM1 puncta. Therefore, the extent of 2-APB inhibition is dependent on relative expression levels of Orai proteins. Indeed, there was one report showing the expression level of Orai proteins is inversely related to 2-APB's ability to reduce STIM1 puncta (20). Thus if enough Orai1 is expressed, after store depletion, all STIM1 molecules would be bound with Orai1, then this powerful Orai1-pushing effect of 2-APB would completely override its inhibition of STIM1 puncta (Fig. 2D) (33).

It has been reported that Orai1 has two STIM1-binding sites (41–43), with its N terminus proposed for channel gating, and its C terminus for STIM1-binding (7, 35, 45). Recently evidence indicates that, both terminus of Orai1 are all involved in STIM1-binding and channel gating (38, 39). It was proposed that 2-APB might compete with STIM1 to gate Orai3 channels (56). Consistent with this idea, 2-APB activated Ca^{2+} influx through Orai1-K85E-V102C is similar to that mediated by STIM1-bound Orai1-K85E-V102C (Red trace in Fig. 5D vs black trace in Fig. 5E). Moreover, we show that pre-incubation with 2-APB could further increase Ca^{2+} influx through STIM1-bound Orai1-V102C (Fig. 5E). And this increase in SOCE activity does not seem to come from alterations in STIM1-binding, as the maximal FRET signals between STIM1 and Orai1-K85E-V102C was unaffected (Fig. 5F). Thus this result indicates that there might be a distinct gating residue in Orai1 channels. Further studies are needed to validate this possibility.

The appearance of STIM1 puncta can reliably indicate the activation of STIM1 (11, 58), thus making STIM1 puncta a very good tool for examining the activation of STIM1 and the developing of STIM1 inhibitors. However, the quantification of STIM1 puncta is often laborious (27). And regular epifluorescent images of STIM1 puncta often blurred by fluorescence contaminations from out of focus signals, thus making it even more difficult to quantify (Fig. 2A vs Fig. 2D). In addition, to obtain confocal or TIRFF measurements of STIM1 puncta, expensive equipment and more training are required. These drawbacks limit the use of STIM1 puncta to monitor STIM1 activation. Here, we show that these above-mentioned limitations are overcome by our recently developed two-component system, which consists of STIM1-(1-310)-CFP and YFP-SOAR or YFP-SOAR-5KQ (13). The activation status of STIM1 can now be easily measured with either co-localization or FRET signals between these two components, making the assessment of drug effects fast and precise (Fig. 1H).

Overall, we provide a valuable two-component tool for examining STIM1 activation. With this tool and other approaches, we clearly dissected and evaluated different inhibitory effects of 2-APB on SOCE, at levels of STIM1, Orai1 and the coupling between these two proteins. Our findings further clarified the molecular basis underling 2-APB's actions. Our strategies

can be applied in future studies examining whether these just identified molecular mechanisms are common to Orai2 and Orai3, to other SOCE inhibitors, especially to those 2-APB analogs. Thus our results may set a good base for better understanding of SOCE activation, and the design of better pharmacological tools for SOCE and future disease therapy.

Acknowledgments

We thank Dr. Yubin Zhou at Texas A&M University Health Science Center for his valuable discussion and insightful suggestions. We thank Dr. Tao Xu and Dr. Pingyong Xu for sharing with us the Orai1-S-S construct. This work was supported by the National Institutes of Health grant (AI058173 and GM109279 to DLG), the National Natural Science foundation of China (NSFC-31471279 to Y.W.), the Recruitment Program for Young Professionals of China (to Y.W.), the Program for New Century Excellent Talents in University (NCET-13-0061 to Y.W.), the American Heart Association SDG grant (13SDG17200006 to S.L.Z.).

References

1. Clapham DE. Calcium signaling. Cell. 1995; 80:259–268. [PubMed: 7834745]
2. Berridge MJ, Lipp P, Bootman MD. The versatility and universality of calcium signalling. Nat Rev Mol Cell Biol. 2000; 1:11–21. [PubMed: 11413485]
3. Parekh AB, Putney JW Jr. Store-operated calcium channels. Physiol Rev. 2005; 85:757–810. [PubMed: 15788710]
4. Wang Y, Deng X, Hewavitharana T, Soboloff J, Gill DL. Stim, ORAI and TRPC channels in the control of calcium entry signals in smooth muscle. Clin Exp Pharmacol Physiol. 2008; 35:1127–1133. [PubMed: 18782202]
5. Soboloff J, Rothberg BS, Madesh M, Gill DL. STIM proteins: dynamic calcium signal transducers. Nat Rev Mol Cell Biol. 2012; 13:549–565. [PubMed: 22914293]
6. Mancarella S, Wang Y, Gill DL. Calcium signals: STIM dynamics mediate spatially unique oscillations. Curr Biol. 2009; 19:R950–952. [PubMed: 19889372]
7. Hogan PG, Lewis RS, Rao A. Molecular basis of calcium signaling in lymphocytes: STIM and ORAI. Annu Rev Immunol. 2010; 28:491–533. [PubMed: 20307213]
8. Vashisht A, Trebak M, Motiani RK. STIM and Orai Proteins as Novel Targets for Cancer Therapy. Am J Physiol Cell Physiol. 2015 ajpcell 00064–02015.
9. Trebak M. STIM/Orai signalling complexes in vascular smooth muscle. J Physiol. 2012; 590:4201–4208. [PubMed: 22641780]
10. Bergmeier W, Weidinger C, Zee I, Feske S. Emerging roles of store-operated Ca(2)(+) entry through STIM and ORAI proteins in immunity, hemostasis and cancer. Channels (Austin). 2013; 7:379–391. [PubMed: 23511024]
11. Hogan PG, Rao A. Store-operated calcium entry: Mechanisms and modulation. Biochem Biophys Res Commun. 2015; 460:40–49. [PubMed: 25998732]
12. Shim AH, Tirado-Lee L, Prakriya M. Structural and functional mechanisms of CRAC channel regulation. J Mol Biol. 2015; 427:77–93. [PubMed: 25284754]
13. Ma G, Wei M, He L, Liu C, Wu B, Zhang SL, Jing J, Liang X, Senes A, Tan P, Li S, Sun A, Bi Y, Zhong L, Si H, Shen Y, Li M, Lee MS, Zhou W, Wang J, Wang Y, Zhou Y. Inside-out Ca(2+) signalling prompted by STIM1 conformational switch. Nat Commun. 2015; 6:7826. [PubMed: 26184105]
14. Palty R, Stanley C, Isacoff EY. Critical role for Orai1 C-terminal domain and TM4 in CRAC channel gating. Cell Res. 2015
15. Putney JW. Pharmacology of store-operated calcium channels. Mol Interv. 2010; 10:209–218. [PubMed: 20729487]
16. Jairaman A, Prakriya M. Molecular pharmacology of store-operated CRAC channels. Channels (Austin). 2013; 7:402–414. [PubMed: 23807116]

17. Prakriya M, Lewis RS. Potentiation and inhibition of Ca(2+) release-activated Ca(2+) channels by 2-aminoethyldiphenyl borate (2-APB) occurs independently of IP(3) receptors. J Physiol. 2001; 536:3–19. [PubMed: 11579153]
18. Ma HT, Venkatachalam K, Parys JB, Gill DL. Modification of store-operated channel coupling and inositol trisphosphate receptor function by 2-aminoethoxydiphenyl borate in DT40 lymphocytes. J Biol Chem. 2002; 277:6915–6922. [PubMed: 11741932]
19. Lis A, Peinelt C, Beck A, Parvez S, Monteilh-Zoller M, Fleig A, Penner R. CRACM1, CRACM2, and CRACM3 are store-operated Ca2+ channels with distinct functional properties. Curr Biol. 2007; 17:794–800. [PubMed: 17442569]
20. DeHaven WI, Smyth JT, Boyles RR, Bird GS, Putney JW Jr. Complex actions of 2-aminoethyldiphenyl borate on store-operated calcium entry. J Biol Chem. 2008; 283:19265–19273. [PubMed: 18487204]
21. Peinelt C, Lis A, Beck A, Fleig A, Penner R. 2-Aminoethoxydiphenyl borate directly facilitates and indirectly inhibits STIM1-dependent gating of CRAC channels. J Physiol. 2008; 586:3061–3073. [PubMed: 18403424]
22. Schindl R, Bergsmann J, Frischauf I, Derler I, Fahrner M, Muik M, Fritsch R, Groschner K, Romanin C. 2-aminoethoxydiphenyl borate alters selectivity of Orai3 channels by increasing their pore size. J Biol Chem. 2008; 283:20261–20267. [PubMed: 18499656]
23. Wang Y, Deng X, Zhou Y, Hendron E, Mancarella S, Ritchie MF, Tang XD, Baba Y, Kurosaki T, Mori Y, Soboloff J, Gill DL. STIM protein coupling in the activation of Orai channels. Proc Natl Acad Sci U S A. 2009; 106:7391–7396. [PubMed: 19376967]
24. Hendron E, Wang X, Zhou Y, Cai X, Goto J, Mikoshiba K, Baba Y, Kurosaki T, Wang Y, Gill DL. Potent functional uncoupling between STIM1 and Orai1 by dimeric 2-aminodiphenyl borinate analogs. Cell Calcium. 2014; 56:482–492. [PubMed: 25459299]
25. Boussif O, Lezoualc'h F, Zanta MA, Mergny MD, Scherman D, Demeneix B, Behr JP. A versatile vector for gene and oligonucleotide transfer into cells in culture and in vivo: polyethylenimine. Proc Natl Acad Sci U S A. 1995; 92:7297–7301. [PubMed: 7638184]
26. Carrasco S, Meyer T. STIM proteins and the endoplasmic reticulum-plasma membrane junctions. Annu Rev Biochem. 2011; 80:973–1000. [PubMed: 21548779]
27. Hewavitharana T, Deng X, Wang Y, Ritchie MF, Girish GV, Soboloff J, Gill DL. Location and function of STIM1 in the activation of Ca2+ entry signals. J Biol Chem. 2008; 283:26252–26262. [PubMed: 18635545]
28. Wang X, Wang Y, Zhou Y, Hendron E, Mancarella S, Andrake MD, Rothberg BS, Soboloff J, Gill DL. Distinct Orai-coupling domains in STIM1 and STIM2 define the Orai-activating site. Nat Commun. 2014; 5:3183. [PubMed: 24492416]
29. Stathopulos PB, Zheng L, Li GY, Plevin MJ, Ikura M. Structural and mechanistic insights into STIM1-mediated initiation of store-operated calcium entry. Cell. 2008; 135:110–122. [PubMed: 18854159]
30. Covington ED, Wu MM, Lewis RS. Essential role for the CRAC activation domain in store-dependent oligomerization of STIM1. Mol Biol Cell. 2010; 21:1897–1907. [PubMed: 20375143]
31. Fahrner M, Muik M, Schindl R, Butorac C, Stathopulos P, Zheng L, Jardin I, Ikura M, Romanin C. A coiled-coil clamp controls both conformation and clustering of stromal interaction molecule 1 (STIM1). J Biol Chem. 2014; 289:33231–33244. [PubMed: 25342749]
32. Navarro-Borelly L, Somasundaram A, Yamashita M, Ren D, Miller RJ, Prakriya M. STIM1-Orai1 interactions and Orai1 conformational changes revealed by live-cell FRET microscopy. J Physiol. 2008; 586:5383–5401. [PubMed: 18832420]
33. Zeng B, Chen GL, Xu SZ. Store-independent pathways for cytosolic STIM1 clustering in the regulation of store-operated Ca(2+) influx. Biochem Pharmacol. 2012; 84:1024–1035. [PubMed: 22842488]
34. Li Z, Liu L, Deng Y, Ji W, Du W, Xu P, Chen L, Xu T. Graded activation of CRAC channel by binding of different numbers of STIM1 to Orai1 subunits. Cell Res. 2011; 21:305–315. [PubMed: 20838418]
35. Zheng H, Zhou MH, Hu C, Kuo E, Peng X, Hu J, Kuo L, Zhang SL. Differential roles of the C and N termini of Orai1 protein in interacting with stromal interaction molecule 1 (STIM1) for Ca2+

release-activated Ca2+ (CRAC) channel activation. J Biol Chem. 2013; 288:11263–11272. [PubMed: 23447534]

36. McNally BA, Somasundaram A, Yamashita M, Prakriya M. Gated regulation of CRAC channel ion selectivity by STIM1. Nature. 2012; 482:241–245. [PubMed: 22278058]
37. Nesin V, Wiley G, Kousi M, Ong EC, Lehmann T, Nicholl DJ, Suri M, Shahrizaila N, Katsanis N, Gaffney PM, Wierenga KJ, Tsiokas L. Activating mutations in STIM1 and ORAI1 cause overlapping syndromes of tubular myopathy and congenital miosis. Proc Natl Acad Sci U S A. 2014; 111:4197–4202. [PubMed: 24591628]
38. Derler I, Plenk P, Fahrner M, Muik M, Jardin I, Schindl R, Gruber HJ, Groschner K, Romanin C. The extended transmembrane Orai1 N-terminal (ETON) region combines binding interface and gate for Orai1 activation by STIM1. J Biol Chem. 2013; 288:29025–29034. [PubMed: 23943619]
39. McNally BA, Somasundaram A, Jairaman A, Yamashita M, Prakriya M. The C- and N-terminal STIM1 binding sites on Orai1 are required for both trapping and gating CRAC channels. J Physiol. 2013; 591:2833–2850. [PubMed: 23613525]
40. Rothberg BS, Wang Y, Gill DL. Orai channel pore properties and gating by STIM: implications from the Orai crystal structure. Sci Signal. 2013; 6:pe9. [PubMed: 23512988]
41. Zhou Y, Meraner P, Kwon HT, Machnes D, Oh-hora M, Zimmer J, Huang Y, Stura A, Rao A, Hogan PG. STIM1 gates the store-operated calcium channel ORAI1 in vitro. Nat Struct Mol Biol. 2010; 17:112–116. [PubMed: 20037597]
42. Park CY, Hoover PJ, Mullins FM, Bachhawat P, Covington ED, Raunser S, Walz T, Garcia KC, Dolmetsch RE, Lewis RS. STIM1 clusters and activates CRAC channels via direct binding of a cytosolic domain to Orai1. Cell. 2009; 136:876–890. [PubMed: 19249086]
43. Hou X, Pedi L, Diver MM, Long SB. Crystal structure of the calcium release-activated calcium channel Orai. Science. 2012; 338:1308–1313. [PubMed: 23180775]
44. Muik M, Frischauf I, Derler I, Fahrner M, Bergsmann J, Eder P, Schindl R, Hesch C, Polzinger B, Fritsch R, Kahr H, Madl J, Gruber H, Groschner K, Romanin C. Dynamic coupling of the putative coiled-coil domain of ORAI1 with STIM1 mediates ORAI1 channel activation. J Biol Chem. 2008; 283:8014–8022. [PubMed: 18187424]
45. Lis A, Zierler S, Peinelt C, Fleig A, Penner R. A single lysine in the N-terminal region of store-operated channels is critical for STIM1-mediated gating. J Gen Physiol. 2010; 136:673–686. [PubMed: 21115697]
46. Muik M, Fahrner M, Schindl R, Stathopulos P, Frischauf I, Derler I, Plenk P, Lackner B, Groschner K, Ikura M, Romanin C. STIM1 couples to ORAI1 via an intramolecular transition into an extended conformation. EMBO J. 2011; 30:1678–1689. [PubMed: 21427704]
47. Gudlur A, Quintana A, Zhou Y, Hirve N, Mahapatra S, Hogan PG. STIM1 triggers a gating rearrangement at the extracellular mouth of the ORAI1 channel. Nat Commun. 2014; 5:5164. [PubMed: 25296861]
48. Moccia F, Zuccolo E, Soda T, Tanzi F, Guerra G, Mapelli L, Lodola F, D'Angelo E. Stim and Orai proteins in neuronal Ca(2+) signaling and excitability. Front Cell Neurosci. 2015; 9:153. [PubMed: 25964739]
49. Shaw PJ, Feske S. Regulation of lymphocyte function by ORAI and STIM proteins in infection and autoimmunity. J Physiol. 2012; 590:4157–4167. [PubMed: 22615435]
50. Yang X, Jin H, Cai X, Li S, Shen Y. Structural and mechanistic insights into the activation of Stromal interaction molecule 1 (STIM1). Proc Natl Acad Sci U S A. 2012; 109:5657–5662. [PubMed: 22451904]
51. Parvez S, Beck A, Peinelt C, Soboloff J, Lis A, Monteilh-Zoller M, Gill DL, Fleig A, Penner R. STIM2 protein mediates distinct store-dependent and store-independent modes of CRAC channel activation. FASEB J. 2008; 22:752–761. [PubMed: 17905723]
52. Amcheslavsky A, Safrina O, Cahalan MD. State-dependent block of Orai3 TM1 and TM3 cysteine mutants: insights into 2-APB activation. J Gen Physiol. 2014; 143:621–631. [PubMed: 24733836]
53. Amcheslavsky A, Safrina O, Cahalan MD. Orai3 TM3 point mutation G158C alters kinetics of 2-APB-induced gating by disulfide bridge formation with TM2 C101. J Gen Physiol. 2013; 142:405–412. [PubMed: 24081982]

54. Yamashita M, Prakriya M. Divergence of Ca(2+) selectivity and equilibrium Ca(2+) blockade in a Ca(2+) release-activated Ca(2+) channel. J Gen Physiol. 2014; 143:325–343. [PubMed: 24567508]
55. Bergsmann J, Derler I, Muik M, Frischauf I, Fahrner M, Pollheimer P, Schwarzinger C, Gruber HJ, Groschner K, Romanin C. Molecular determinants within N terminus of Orai3 protein that control channel activation and gating. J Biol Chem. 2011; 286:31565–31575. [PubMed: 21724845]
56. Yamashita M, Somasundaram A, Prakriya M. Competitive modulation of Ca2+ release-activated Ca2+ channel gating by STIM1 and 2-aminoethyldiphenyl borate. J Biol Chem. 2011; 286:9429–9442. [PubMed: 21193399]
57. Prakriya M, Lewis RS. Regulation of CRAC channel activity by recruitment of silent channels to a high open-probability gating mode. J Gen Physiol. 2006; 128:373–386. [PubMed: 16940559]
58. Liou J, Kim ML, Heo WD, Jones JT, Myers JW, Ferrell JE Jr, Meyer T. STIM is a Ca2+ sensor essential for Ca2+-store-depletion-triggered Ca2+ influx. Curr Biol. 2005; 15:1235–1241. [PubMed: 16005298]

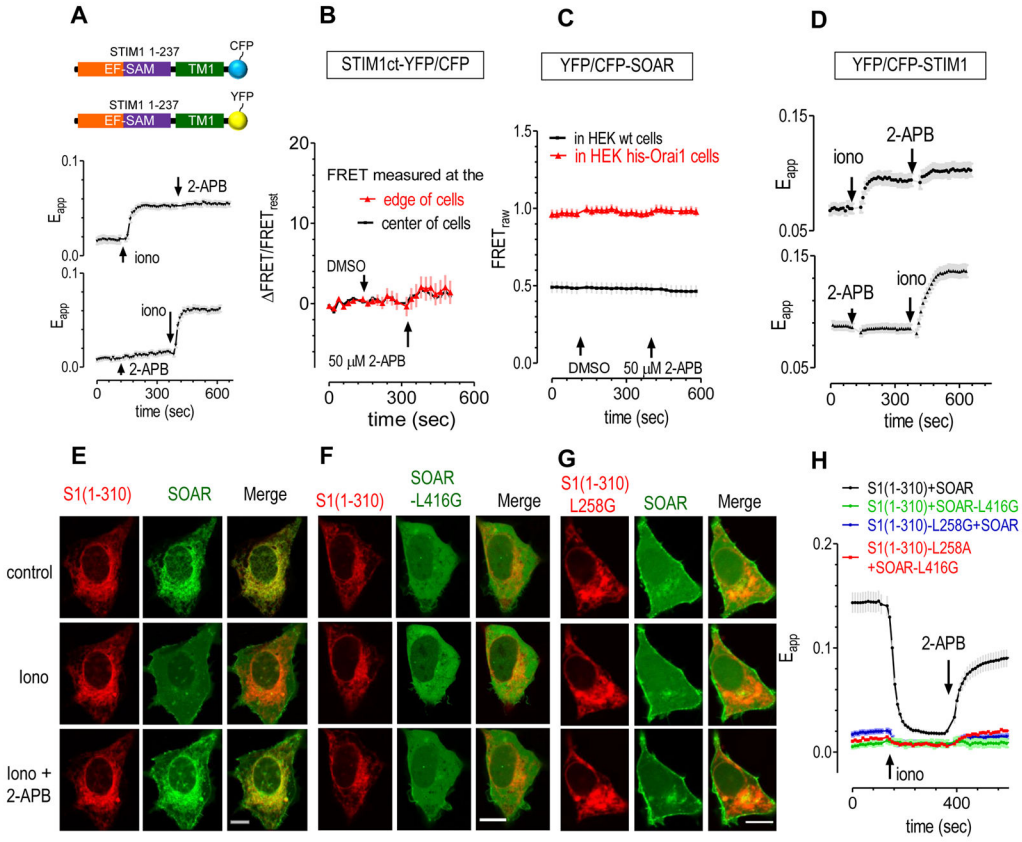

Figure 1. 2-APB has no effect on STIM1-STIM1 interactions, but enhanced intramolecular interactions between STIM1-CC1 and SOAR region

(A) In HEK wt cells transiently co-expressing STIM1-(1-237)-CFP or STIM1-(1-237) -YFP, 2-APB didn't induce any detectable changes in FRET signals between these two proteins regardless of store status. Upper trace: 2-APB was applied after ionomycin. Lower trace: 2-APB was applied before ionomycin. (B) 2-APB didn't induce any detectable changes in FRET signals between STIM1ct-YFP and STIM1ct-CFP that were transiently co-expressed in HEK wt cells. (C) 2-APB had no effect on FRET signals between YFP- and CFP-SOAR transiently co-expressed in HEK wt or his-Orai1 cells. (D) In HEK wt cells transiently co-expressing YFP-STIM1 or CFP-STIM1, ionomycin-induced FRET changes were unaffected by 2-APB, no matter is applied after ionomycin (upper figure) or before store depletion (bottom figure). (E–H) In HEK wt cells co-expressing STIM1-(1-310)-CFP and YFP-SOAR or their corresponding mutants, after ER calcium store were depleted with ionomycin (2.5 μM), effects of 2-APB (50 μM) on these STIM1 mutants were tested. Images shown here were collected with confocal imaging (scale bar, 10 μm). (E) 2-APB partially reversed the ionomycin-diminished co-localization between STIM1-(1-310) and SOAR. (F) STIM1-L416G lost its ability to co-localize with STIM1-(1-310), and 2-APB cannot make STIM1-L416G co-localize with STIM1-(1-310). (G) Similarly, STIM1-(1-310)-L258G mutant abolished ionomycin or 2-APB induced changes in co-localizations between STIM1-(1-310)-L258G and SOAR. (H) The effects of ionomycin or 2-APB on the FRET signals between STIM1-(1-310)-CFP and YFP-SOAR or their corresponding mutants were examined. 2-APB could partially reverse the ionomycin-induced decreases in FRET signals

between wt STIM1-(1-310) and wt SOAR. STIM1-(1-310)-L258G or SOAR-L416 abolished these effects induced by ionomycin or 2-APB

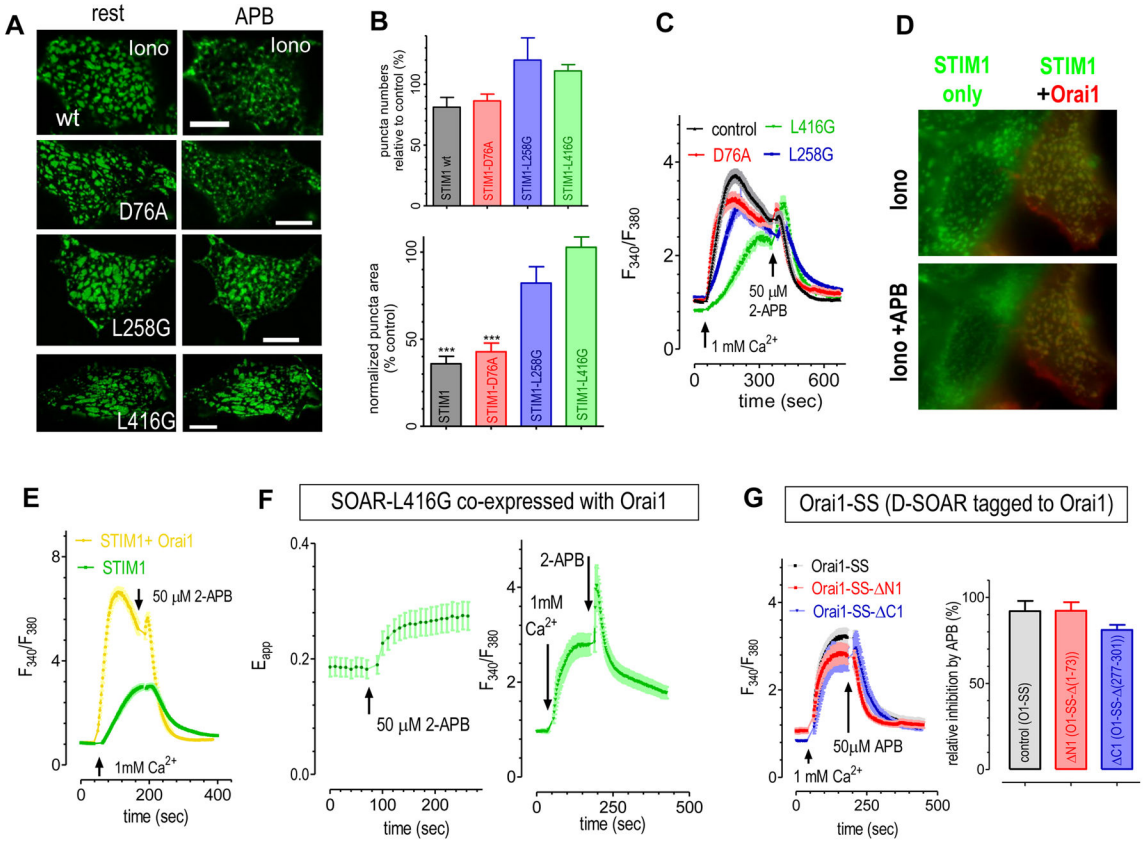

Figure 2. After abolishing its inhibitory effect on STIM1 or STIM1 puncta, 2-APB can still inhibit Ca^{2+} influxes that are mediated by various types of STIM1/Orai1 complexes

Intracellular Ca^{2+} signals were measured with Fura-2, a ratio metric Ca^{2+} indicator. (A–C) In HEK wt cells transiently expressing wt STIM1 or its various mutants (wt STIM1; STIM1-D76A; STIM1-L258G; or STIM1-L416G), 2-APB's effects on ionomycin-induced or constitutive puncta (A–B) or corresponding Ca^{2+} influx (C) were examined. (A) Punctate images taken with confocal microscopy. Puncta formed by wt STIM1 or STIM1-D76A were both inhibited by 2-APB, while constitutive puncta formed by STIM1-L258G or STIM1-L416G were not significantly affected. (Scale bar: 10 μm). (B) Statistics of figure (A). Top image: effects on puncta number ($p>0.06$, paired t-test, $n>=6$). Bottom image: effect of 2-APB on mean punctate area (***, Paired T-test, $p<0.001$). (C) 2-APB inhibited Ca^{2+} influxes similarly in cells expressing wt STIM1 or different STIM1 mutants. (D–E) Even though 2-APB cannot reverse puncta formation in HEK STIM1-Orai1 cells (the orange cell in left figure), it can inhibit SOCE in both HEK STIM1 and HEK STIM1-Orai1 cells. To aid comparison, two types of stable cells were seeded on the same coverslip: HEK stable cells co-expressing just STIM1-YFP (green trace), or both STIM1-YFP and Orai1-CFP (orange trace), and the effects of 2-APB on STIM1-puncta (D) or SOCE (E) were examined. Images were obtained with regular epifluorescence microscopy. (F) In HEK Orai1-CFP cells transiently expressing YFP-SOAR-L416G, 2-APB increased the FRET signals (left figure), but inhibited the Ca^{2+} entry (right figure), even though both processes are both mediated by these two proteins. (G) In HEK wt cells transiently expressing eGFP-Orai1-SS, or its

corresponding ΔN1(Δ1-73), ΔC1(Δ277-301) mutants. Constitutive Ca^{2+} entry were similarly inhibited by 2-APB. Left: typical traces; right: statistics.

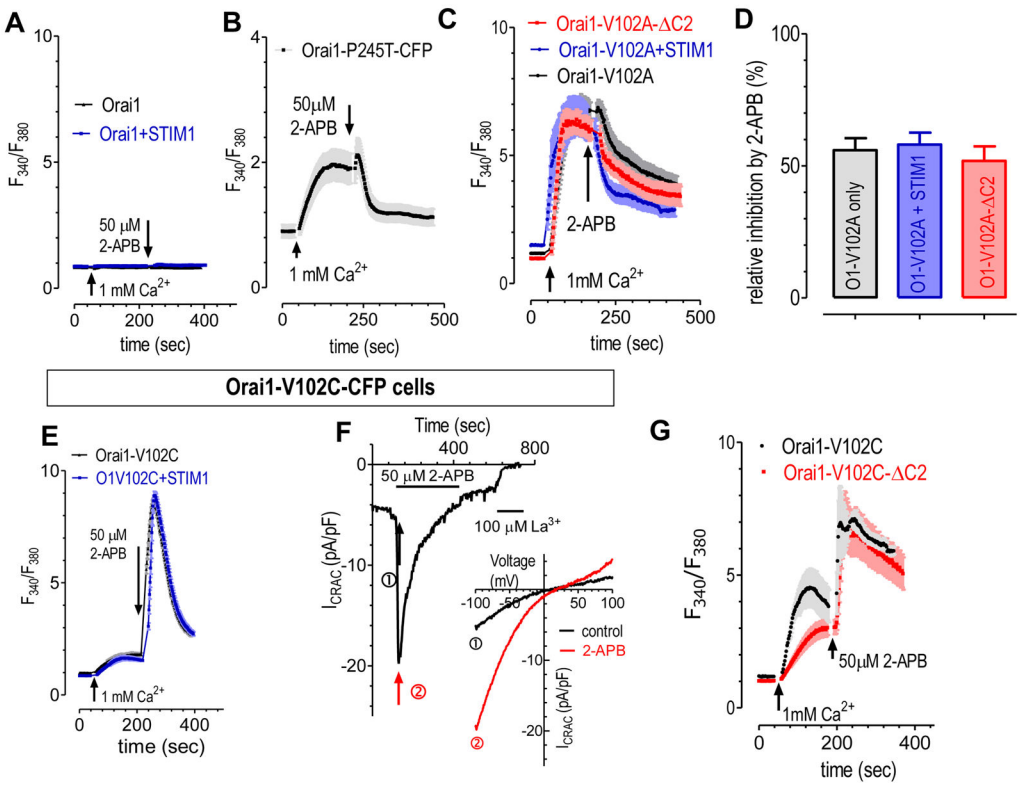

Figure 3. 2-APB can directly enhance or inhibit constitutive Ca^{2+} influx that are mediated by Orai1 mutants

Intracellular Ca^{2+} signals were measured with a ratio metric Ca^{2+} indicator, Fura-2. All 2-APB (50 μM) treatments were carried out when ER Ca^{2+} store was full. (A) 2-APB didn't induce Ca^{2+} entry in HEK Orai1, or STIM1-Orai1 stable cells. (B) In HEK we cells transiently expressing Orai1-P245T-CFP, constitutive Ca^{2+} influxes mediated by Orai1-P245T were greatly inhibited by 2-APB. (C–D) In HEK wt cells transiently expressing Orai1-V102A, Orai1-V102A together with STIM1, or Orai1-V102A-ΔC2 (Δ267-301), 2-APB similarly inhibited constitutive Ca^{2+} entry through Orai1-V102A. (C), representative curve; (D), statistics. (E) In HEK Orai1-V102C-CFP cells, constitutive Ca^{2+} influxes mediated by Orai1-V102C were greatly enhanced by 2-APB. And overexpression of STIM1-YFP has no effect on constitutive or 2-APB induced Ca^{2+} entry. (F) 2-APB enhanced whole cell current in HEK Orai1-V102C cells. Insert: I–V relationship measured at time points indicated by arrows. To avoid passive store depletion, pipette solution contained 100nM free Ca^{2+} and 2mM ATP. (G) 2-APB enhanced constitutive Ca^{2+} influxes similarly in HEK wt cells transiently expressing Orai1-V102C or its mutant devoid of STIM1 binding, Orai1-Δ(267-301).

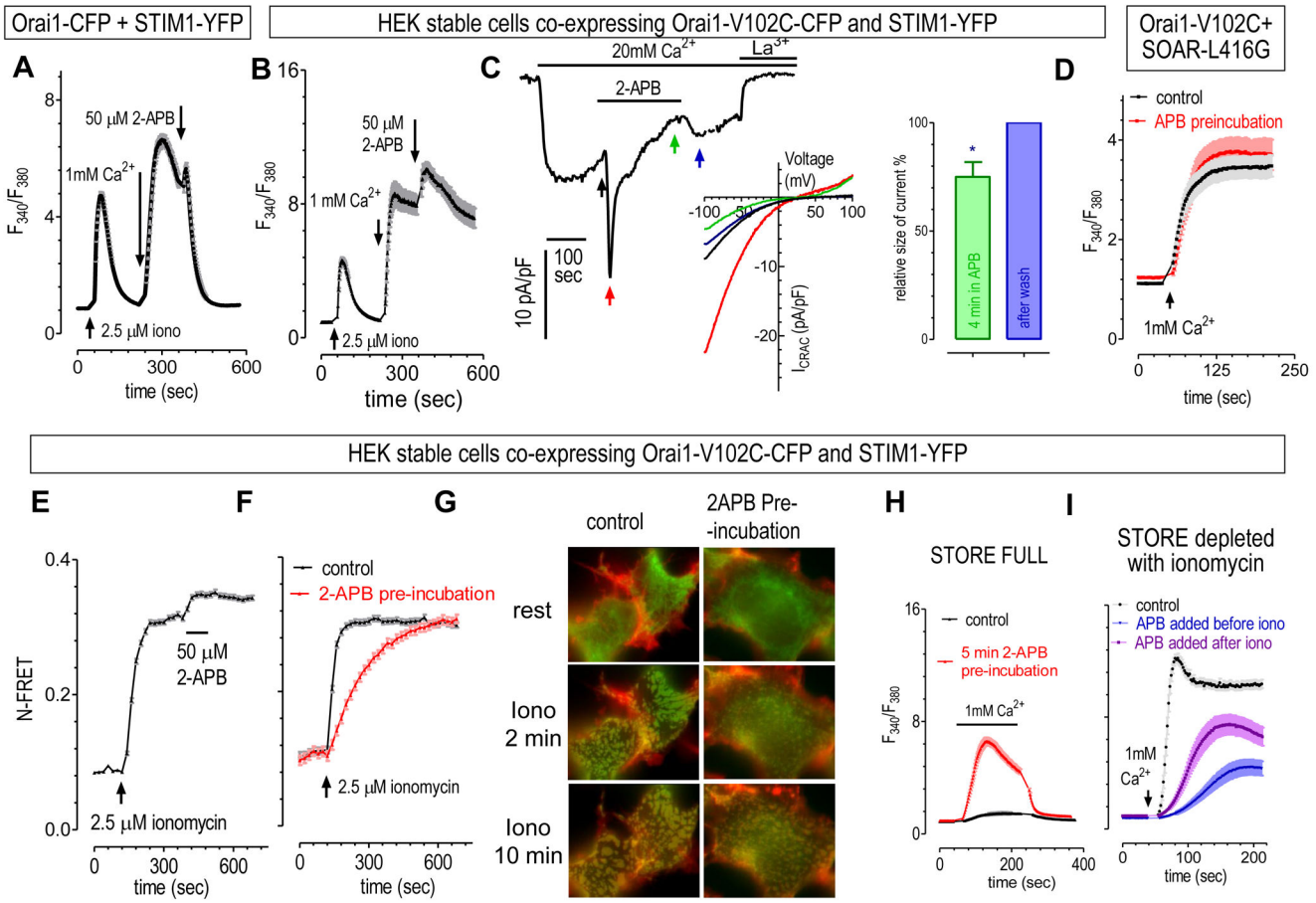

Figure 4. 2-APB's inhibition on STIM1 also slowly contributes to its inhibitory effect on SOCE

Unless specified, all other experiments were carried out in HEK stable cells co-expressing Orai1-V102C-CFP and STIM1-YFP. And ER Ca^{2+} store were depleted with 2.5 μM ionomycin in all imaging experiments. Intracellular Ca^{2+} levels were shown as Fura-2 ratio signals. Concentration of 2-APB was 50 μM. (A) In HEK stable cells co-expressing STIM1-YFP and Orai1-CFP, after a transient activation, 2-APB quickly inhibited SOCE mediated by STIM1 and Orai1. (B) In HEK STIM1+Orai1-V102C stable cells, ionomycin-induced Ca^{2+} entry was transiently enhanced by 2-APB, while the effect of inhibitions was not very obvious. (C) 2-APB first transiently enhanced I_{CRAC} mediated by STIM1 and Orai1-V102C, and then it slowly inhibited I_{CRAC}. Left: development of whole-cell current in a typical cell; middle: I–V relationships of the same cell in left figure at various time points as indicated by arrows. ER Ca^{2+} store in patched cells was passively depleted by including 20mM EGTA in pipette solution; right: Statistics showing the recovery of current after the removal of 2-APB from bath solution. Currents in the presence of 2-APB (indicated by green arrow) were normalized against peak current after the removal of 2-APB (indicated by blue arrow). (p=0.02, paired T-test, n=6). (D) In HEK Tsa cells transiently expressing YFP-SOAR-L416G and Orai1-V102C-CFP, 5 min pre-incubation of 2-APB has no effect on Ca^{2+} entry mediated by these two proteins. (E) 2-APB further increased FRET signals between STIM1 and Orai1-V102C after store depletion. (F) 5 min pre-incubation with 2-APB slowed down the rate of increase in FRET signals between STIM1 and Orai1-V102C. (G) Compared to

control, 5 min pre-incubation with 2-APB slowed down the appearance of STIM1 puncta, examined with epifluorescence imaging. (H) When ER Ca^{2+} store is full, 5 min incubation with 2-APB only enhances the constitutive Ca^{2+} influx. (I) 5 min pre-incubation with 2-APB greatly inhibited SOCE after store depletion. When 2-APB was applied before store depletion, the inhibitory effect is greater than those applied after store depletion.

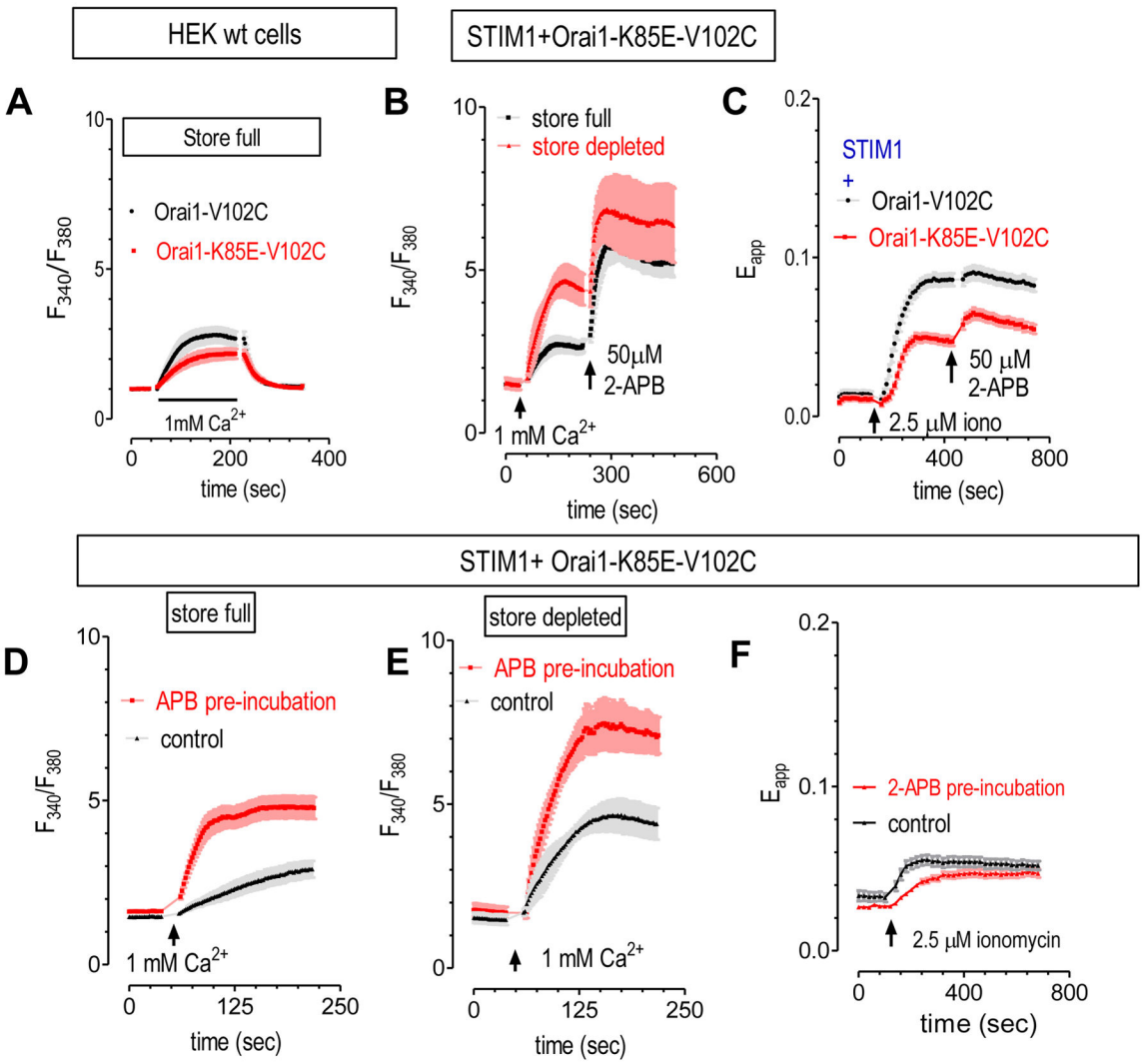

Figure 5. K85E mutation abolished 2-APB's inhibition on STIM1-bound Orai1-V102C STIM1-Orai1

Except for the first figure, all other experiments were carried out in HEK SITM1-YFP stable cells transiently expressing Orai1-V102C-CFP, or its K85E mutant. 2.5 μM ionomycin were used for store depletion, and the effects of 2-APB (50 μM) were examined. Intracellular Ca^{2+} levels were examined with Fura-2 indicator. (A) When transiently expressed in HEK wt cells, K85E mutation (red trace) decreases the resulting constitutive Ca^{2+} entry as compared to control (black trace). (B) When applied after the addition of Ca^{2+}, 2-APB enhanced the Ca^{2+} responses mediated by Orai1-K85E-V102C, no matter the ER store is full (black trace) or depleted (red trace). (C) Compared to control (black trace), K85E mutation (red trace) reduced ionomycin-induced increases in FRET signals between STIM1 and Orai1-V102C. (D–F) When 2-APB is applied 5 min before store depletion with ionomycin, both (D) constitutive Ca^{2+} entry and (E) SOCE were enhanced. (F) While the rate of ionomycin-induced increase in FRET signals between STIM1 and Orai1-K85E-V102C was slowed down.